Electronic Supplementary Material

A molecular dynamics study on the tribological behavior of molybdenum disulfide with grain boundary defects during scratching processes

Boyu WEI[1], Ning KONG[1,*], Jie ZHANG[1], Hongbo LI[1], Zhenjun HONG[1], Hongtao ZHU[2], Yuan ZHUANG[3], Bo WANG[3]

[1]*School of Mechanical Engineering, University of Science and Technology Beijing, Beijing 100083, China*

[2]*School of Mechanical, Materials & Mechatronics Engineering, University of Wollongong, Wollongong, NSW 2522, Australia*

[3]*Beijing Institute of Spacecraft System Engineering, Beijing 100094, China*

Supporting information to https://doi.org/10.1007/s40544-020-0459-z

1 Thermosetting scheme

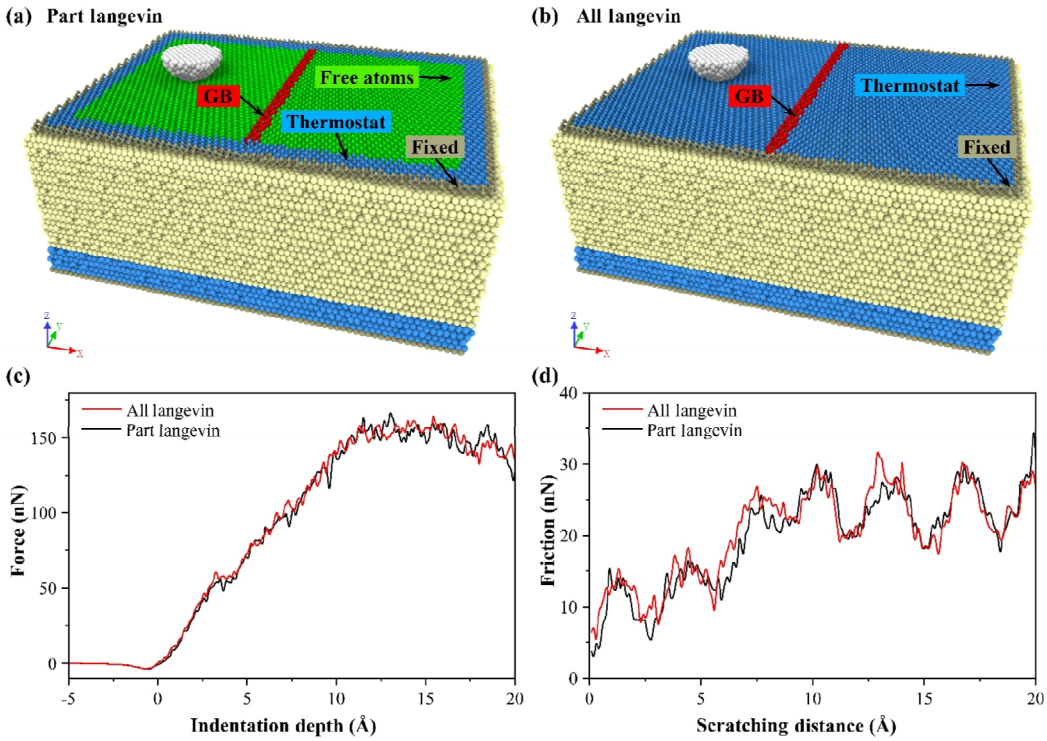

Fig. S1 Schematic of two thermostat schemes: (a) Part Langevin (the Langevin thermostat is only applied to the MoS_2 atoms close to the fixed region) and (b) All Langevin (the Langevin thermostat is applied to all free atoms from the MoS_2 layer). Part Langevin is adopted in this work. For both schemes, the thermosetting regions in the Pt substrate are the same as that in the main manuscript. (c) Force–depth relations of the MoS_2/Pt substrate during nano-indentation process using Part Langevin and All Langevin. (d) Friction–distance curves of the MoS_2/Pt substrate during nano-scratch process using Part Langevin and All Langevin. The thermostat scheme in this work does not show artificial effects on the simulation results.

* Corresponding author: Ning KONG, E-mail: kongning@ustb.edu.cn

2 Model

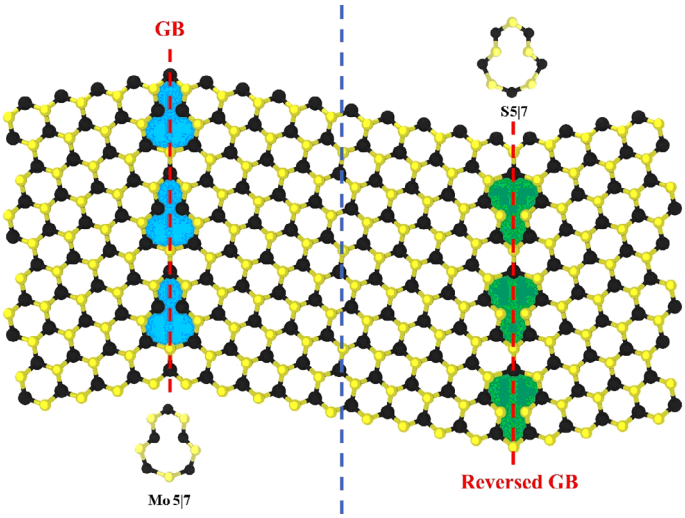

Fig. S2 Schematic of the GB consisting of Mo5|7 dislocation cores and the reversed GB consisting of S5|7 dislocation cores.

3 The parameters of LJ potentials

Table S1 Parameters of LJ potentials used in the simulation.

Parameter	ε (meV)	σ (Å)	Rcutoff (Å)
C–S	13.165	3.418	8.545
C–Mo	48.962	3.009	7.523
C–Pt	38.635	2.971	7.428
S–Pt	177.840	2.922	7.305
Mo–Pt	661.41	2.513	6.283

4 Indentation points and scratching lines

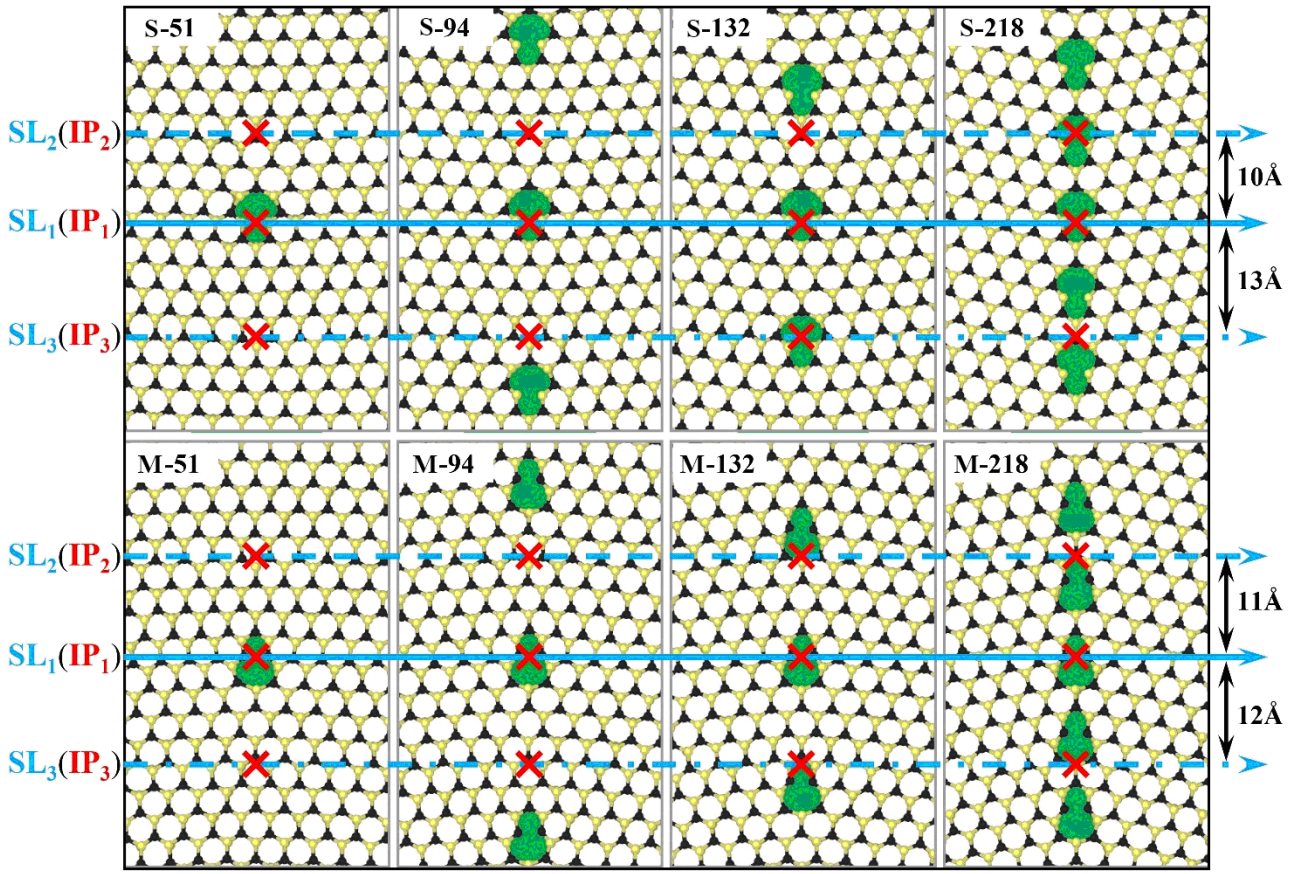

Fig. S3 Schematic of indentation points (IP) and scratching lines (SL) on the MoS_2. Without further mention, the results in this manuscript are based on scratching line 1 (SL_1) and indentation point 1 (IP_1).

5 Critical normal load of indentation and scratching

Table S2 Critical normal loads of indentation and scratching.

Model	Critical normal load of indentation (nN)				Critical normal load of scratching (nN)			
	IP_1	IP_2	IP_2	AVE	SL_1	SL_2	SL_3	AVE
S-51	78.65	74.31	80.09	77.68	68.51	62.37	65.24	65.37
S-94	83.40	78.69	84.17	82.09	77.83	70.29	74.75	74.29
S-132	89.11	88.25	85.33	87.56	79.21	77.09	77.98	78.09
S-218	90.33	93.64	95.34	93.10	82.57	81.69	86.80	83.69
M-51	87.21	81.47	89.16	85.95	73.45	69.77	75.09	72.77
M-94	89.43	85.29	92.82	89.18	79.77	75.66	77.56	77.66
M-132	90.40	93.11	95.31	92.94	84.16	80.94	83.71	82.94
M-218	99.50	98.65	99.78	99.31	89.63	87.40	91.16	89.40

6 Combined effect of pushing and interlocking actions

Table S3 Interaction force between the specific tip atoms and MoS_2 atoms in M-51 model.

Time (ps)	Interaction	*X* component (nN)	*Y* component (nN)	Angle (°)	Resultant force (nN)
445	A → 1	–2.32	1.26	151.50	2.64
	A → 2	3.07	0.61	11.24	3.13
	B → 3	0.96	2.68	70.32	2.85
470	A → 2	1.13	4.63	76.30	4.77
	B → 3	–0.87	0.81	136.98	1.19
	B → 4	4.22	2.11	26.61	4.72
505	C → 5	–0.53	–0.76	–124.74	0.93
	C → 6	0.47	–1.04	–65.65	1.14

Table S4 Interaction force between the specific tip atoms and MoS_2 atoms in S-51 model.

Time (ps)	Interaction	*X* component (nN)	*Y* component (nN)	Angle (°)	Resultant force (nN)
430	A → 1	3.12	1.99	32.52	3.7
	A → 3	1.37	2.56	–61.81	2.9
455	A → 2	2.11	1.52	35.75	2.6
	C → 5	1.89	1.48	–38.05	2.4
505	C → 6	1.95	2.41	–51.02	3.1

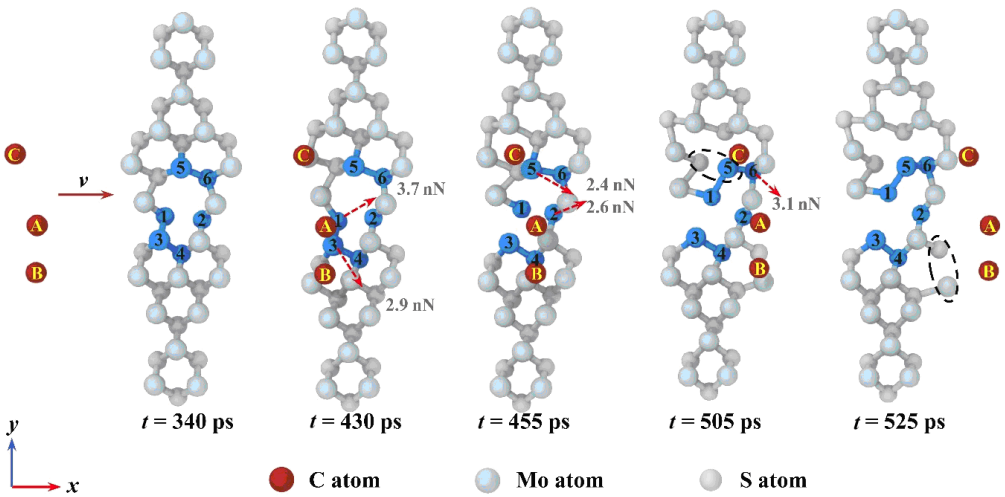

Fig. S4 Schematic of the specific tip atoms and MoS_2 atoms of S-51 Model during the scratching process at the load depth of 5.1 Å. The representative atoms and bonds were marked by blue color, black dotted circles, and red dashed arrows to help tracking the bond-breaking process.

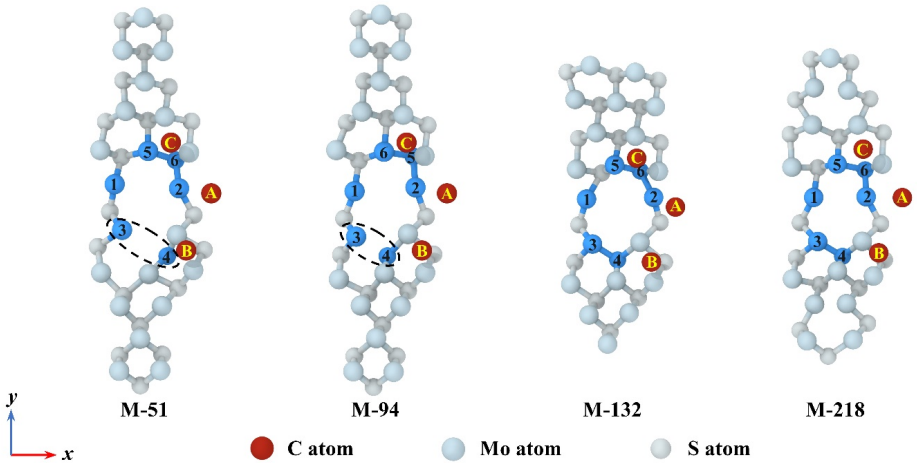

Fig. S5 Schematic of the specific tip atoms and MoS_2 atoms of Mo5|7 cores-containing models when the scratching time is 505 ps at the load depth of 5.4 Å. The top S layer is hidden to show the structural changes of MoS_2 clearly. The representative atoms of the tip and MoS_2 were marked by red and blue color, respectively. The broken bonds were marked by black circle.

7 The tribological behavior of GB defects-containing MoS_2

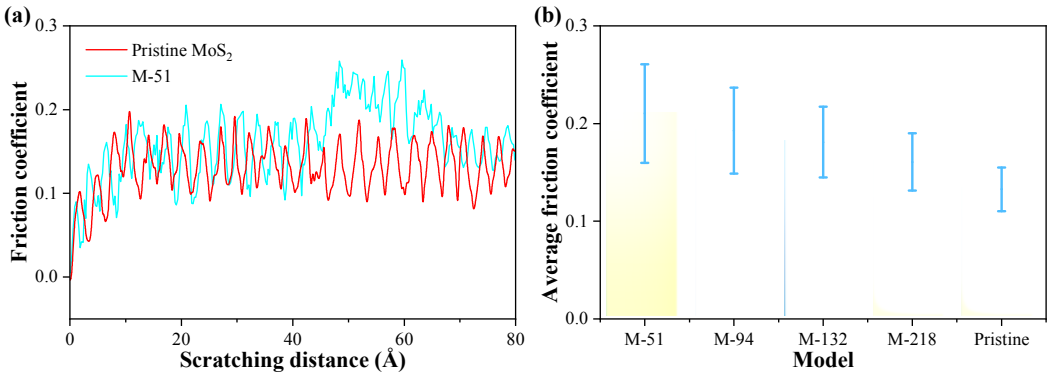

Fig. S6 (a) Relationship between friction coefficient and scratching depth and (b) average friction coefficient of pristine MoS_2 and Mo5|7 cores-containing models at a scratching depth of 5.4 Å.

8 Wear mechanism of MoS_2 with S5|7-containing GB defects

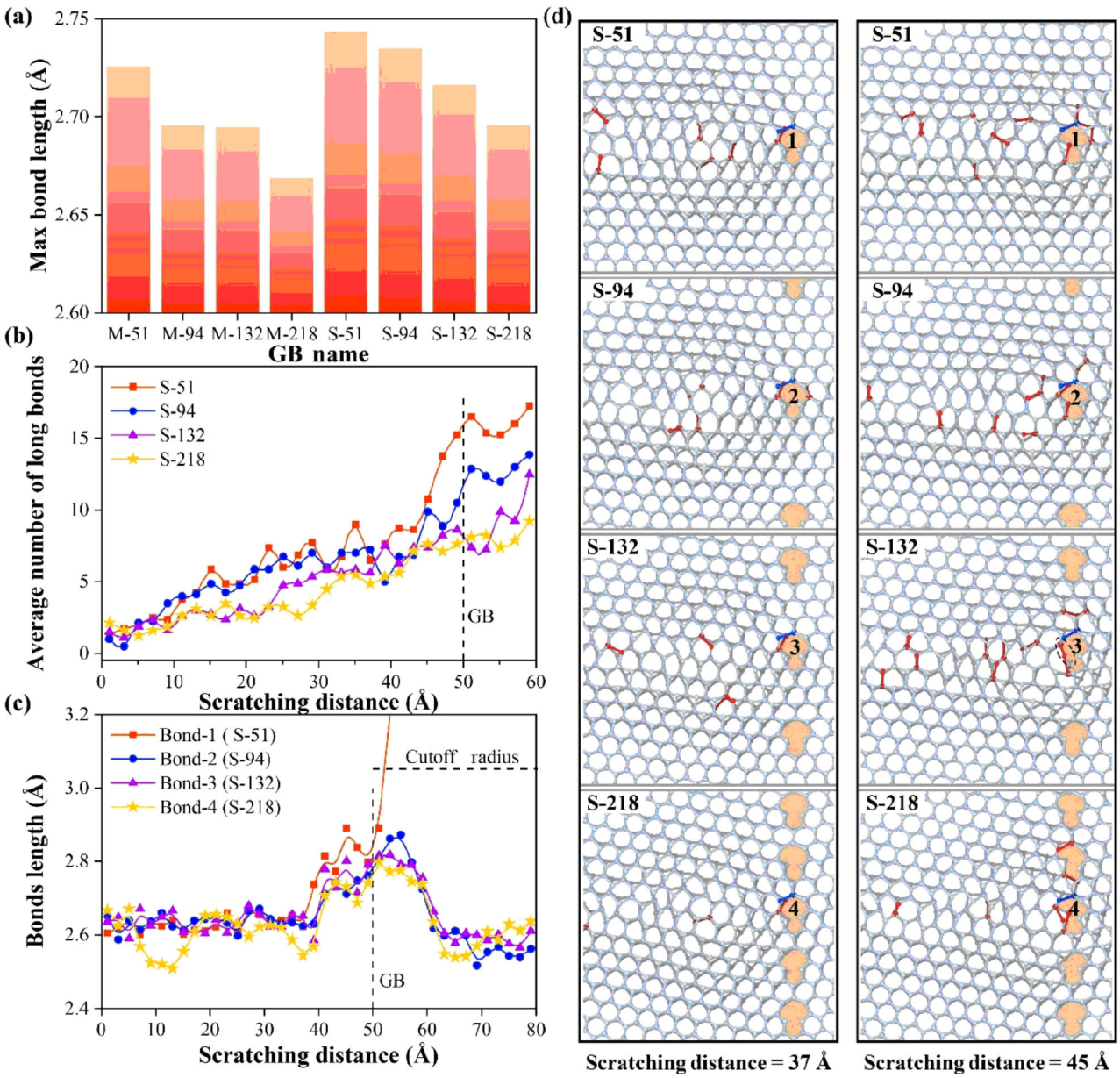

Fig. S7 (a) Longest pre-strain Mo–S bond length of Mo5|7 and S5|7 cores-containing models at equilibrium. (b) Average number of long Mo–S bonds as a function of the scratching distance before MoS_2 starts to break in S-51 model. The number of long bonds is averaged with an interval of 1 Å. The diamond tip is positioned at an initial distance of 50 Å from the GB along the *x* direction. (c) Relationship between the length of the critical bond 1–4 and scratching distance. (d) At the load depth of 5.1 Å, the distributions of the long Mo–S bonds for S-51, S-94, S-132, and S-218 models at two sliding distances of 37 and 45 Å, respectively. The long Mo–S bonds are marked in red, and the S5|7 defects along the GBs are colored in bisque. The critical bonds within GBs are numbered by 1–4 and highlighted in blue.

9 Weakening the negative effects of GB defects on the tribological properties of MoS_2

Table S5 Work of adhesion for M-51 and S-51 models with different LJ parameters.

	Work of adhesion for M-51 (J/m^2)	Work of adhesion for S-51 (J/m^2)
LJ-1	1.0283	1.0295
LJ-2	1.5674	1.5667
LJ-3	2.1305	2.1290
LJ-4	2.6440	2.6428

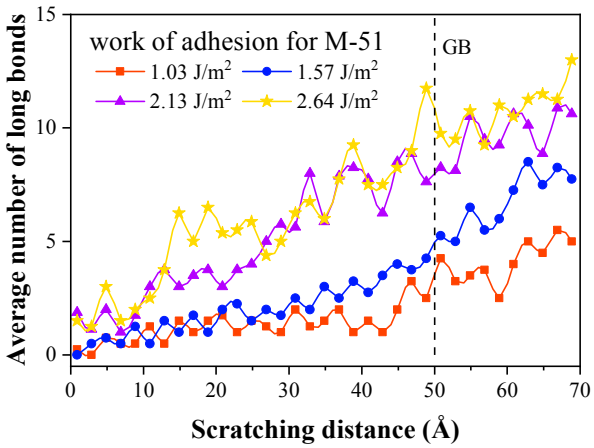

Fig. S8 Average number of the long Mo–S bonds of M-51 model with different adhesive strengths at the load depth of 4.9 Å.